Numerical Analysis of Impact Deformation and Failure in Composite Plates

ALEXANDER E. BOGDANOVICH AND ENDEL V. IARVE*
Engineering and Technology Center
Latvian Academy of Sciences
Latvia
U.S.S.R.

(Received June 18, 1990)
(Revised April 9, 1991)

ABSTRACT: The analytical problem of transverse impact by a rigid body on a rectangular composite plate is considered. The calculation of displacements, deformations and stresses in conjunction with the characteristics of impact contact interaction is provided. The analysis of transverse stresses arising under short-time impulse in graphite/epoxy and organic glass/polymeric adhesive laminated plates is performed. The results illustrating dependencies of a contact force on time are given for various levels of mass and velocity of the impactor at the prescribed impact energy. The analysis of impact damage zones in a three-ply and a five-ply graphite/epoxy laminate (particularly, having soft polymeric interleaves) is presented for the case of 2–2.5 J impact energy and different mass and velocity combinations. The changing of the failure mode increasing the impactor velocity (decreasing the mass) is followed up.

INTRODUCTION

THE THEORY OF deformation and failure of composite plates subjected to transverse low velocity impact, remains to be rather undeveloped. A great majority of papers devoted to this subject are based on the theories of thin anisotropic plates which don't allow accounting for stress wave propagation processes through the thickness, and accordingly analyzing all the typical impact failure modes described in experimental works. The principal necessity is to take into account the structural inhomogeneity of the plate, namely the mechanical inhomogeneity of reinforced materials and the presence of layers having different mechanical characteristics. These require that special approaches to the analyses would be elaborated. For example, solving the problem of the theory of elasticity in terms of displacements, using finite element or finite difference methods, one

*Visiting Scientist for AdTech Systems Research, Inc., 1342 North Fairfield Rd., Dayton, OH 45432, U.S.A.

0021-9983/92/04 0520-26 $6.00/0

is to add certain special procedures to calculate the interlaminar stresses. The alternative approach, based on a hybrid finite element with independent approximations of displacements and stresses, leads to higher-order systems of equations and requires extensive computer time and resources. Therefore, some new ideas are required to elaborate more efficient numerical methods to handle different dynamic problems of laminated composite structural elements.

To consider the impact problem, a certain theoretical model to describe the dynamic contact interaction is needed. Three different levels of this model can be selected from the literature. The most simple way is to reduce the problem of obtaining the response characteristics of the plate under an impulse of normal pressure. The duration of the impulse and the amplitude of the pressure depend on the mass and velocity of the impactor and elastic properties of the plate. To establish these relations can be used the experimental data or simple theoretical models like impact on a half-space using the classic Herz's formula. The application of this approach is restricted by rather low impactor velocities when the impact time is much longer than the period of eigen vibrations of the plate at the main mode. The discussion and numerous applications of this approach can be found in Reference [6].

The most popular is probably the approach introduced by S. P. Timoshenko. He considered the normal transverse impact of a steel ball at steel beam. According to him the normal displacement of the ball is a sum of two terms. They are the deflection of the beam and local penetration. The latter term can be evaluated using the classic Hertz's formula. A valuable step in the application of this approach to composites was made in References [7–9]. In Reference [7] it was stated that the crater on impacted surface can be easily created in the case of graphite/epoxy plates even at comparatively low impact velocities, and therefore, it is more realistic to use the contact law [7] instead of Hertz's contact law. Otherwise, we can note that there are experimental data [10], for example, that reveal certain fundamental distinctions in the deformation processes for thermoset and thermoplastic graphite composites at low velocity impact loading. One of them is the creation of a small dent on the impacted surface of thermoplastic composites and absence of visible damages on the same surface of thermoset composites up to the start of cracking on the opposite surface. In a great number of experimental works for different graphite composites, it was stated that in the range of impact energy up to 5 J, the typical are invisible or barely visible from the impacted surface internal damages. It is obvious that the universal contact law is to take into account both the plastic deformation and the cracking of matrix in the vicinity of indentor. It seems very complicated to formulate such a law in a correct mathematical way and, moreover, to use it in practical calculations. The general restriction of this kind of model, based on quasi-static impact interaction simulation, is that the interaction time used to be substantially greater than the time of a one-way run of a stress wave through the characteristic size of a target body (in particular, its thickness).

The more general and, correspondingly, more complex approach for solving the problem of impact-contact interaction, is based on a formulation of the joint dynamic contact problem for the system "impactor-target." There are two versions of such an approach known from the literature. The first one is tightly connected with the particular numerical method to be applied: finite element or finite difference method [11]. The second is based on some variational principles [12] and seems to be more promising for complex dynamic contact problems. It is worth noting that particular numerical results have been obtained by use of both of these approaches only for rather simple three-dimensional quasi-static and two-dimensional dynamic problems.

The other significant problem is to calculate the stress-strain state in a plate during the impact loading. For the detailed impact failure analysis, an approach based on the equations of three-dimensional theory of elasticity for laminated anisotropic media [13–16] is needed. In Reference [13] the numerical solution based on 8-node rectangular finite element was elaborated. An impact interaction problem was reduced to the loading by a prescribed surface pressure impulse. In References [14–16] the same numerical approach was used together with the contact interaction law [7]. The most interesting in Reference [14] is the analysis of the location and the size of delaminations. The calculated "map of delaminations" is compared to the experimental results [13] and a very good agreement between these results is obtained. For the same purpose, a combination of two failure criteria—tensor-polynomial for in-ply failure and Hashin's criteria for interlaminar failure, were presented in Reference [15]. The strain energy density as a function of time was calculated in Reference [16] on the basis of the finite element. The results obtained for various ply orientations in a laminate revealed that the strain energy propagates considerably faster in the direction of reinforcement than in transversal directions. These results correspond to the experimental fact that impact damage zones are strictly extended in the direction of reinforcement. It was also stated in Reference [16] that distribution of strain energy density through the thickness depends substantially on the structure of a laminate. The possibility of an analytical prediction of different types of damages in a graphite/epoxy laminate was illustrated in Reference [3]. In the following sections, we shall continue to discuss this subject, emphasizing the fact that it is not sufficient to operate with impact energy only. Both the parameters, mass and velocity which form the prescribed impact energy, are of a great importance.

PROBLEM FORMULATION

Let us consider first the calculation of displacements strains and stresses in a multilayered orthotropic plate under the impulse surface load [Figure 1(a)]. Rectangular plate of length L in the x-direction, width A in the y-direction and thickness H is considered and is located in $0xyz$ coordinates to occupy the region $[0,L]*[0,A]*[0,H]$. The plate consists of n orthotropic layers. In each layer the orientation of principal material axis is defined relative to the x-axis and denoted θ_k, $k = 1,\ldots,n$. The 3-D linear dynamic problem is formulated. The strain components are expressed through the displacement components $u_x(x,y,z,t)$, $u_y(x,y,z,t)$, $u_z(x,y,z,t)$ in the form

$$\epsilon_{xx} = \frac{\partial u_x}{\partial x} \qquad \epsilon_{yy} = \frac{\partial u_y}{\partial y} \qquad \epsilon_{zz} = \frac{\partial u_z}{\partial z} \tag{1}$$

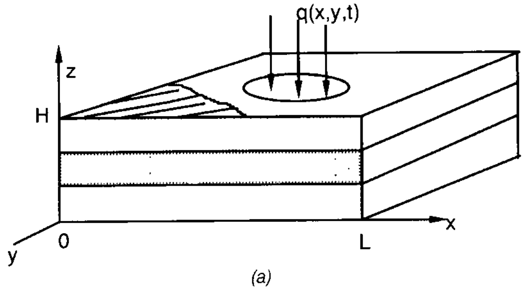

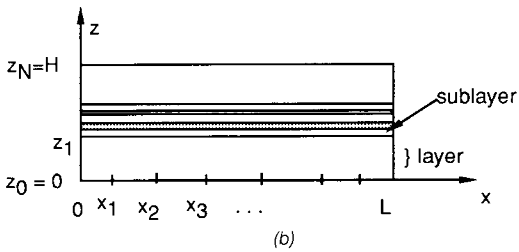

Figure 1. *Multilayered plate, coordinate system (a); division into sublayers in z-direction and intervals in x-direction (b).*

$$\gamma_{yz} = \frac{\partial u_y}{\partial z} + \frac{\partial u_z}{\partial y} \qquad \gamma_{xz} = \frac{\partial u_x}{\partial z} + \frac{\partial u_z}{\partial x} \qquad \gamma_{yx} = \frac{\partial u_y}{\partial x} + \frac{\partial u_x}{\partial y}$$

In a certain layer, with respect to $0xyz$-coordinates, the stress-strain relations can be written

$$\begin{aligned}
\sigma_{xx}^{(k)} &= \bar{Q}_{11}^{(k)}\epsilon_{xx} + \bar{Q}_{12}^{(k)}\epsilon_{yy} + \bar{Q}_{13}^{(k)}\epsilon_{zz} + \bar{Q}_{16}^{(k)}\gamma_{xy} \\
\sigma_{yy}^{(k)} &= \bar{Q}_{21}^{(k)}\epsilon_{xx} + \bar{Q}_{22}^{(k)}\epsilon_{yy} + \bar{Q}_{23}^{(k)}\epsilon_{zz} + \bar{Q}_{26}^{(k)}\gamma_{xy} \\
\sigma_{zz}^{(k)} &= \bar{Q}_{31}^{(k)}\epsilon_{xx} + \bar{Q}_{32}^{(k)}\epsilon_{yy} + \bar{Q}_{33}^{(k)}\epsilon_{zz} + \bar{Q}_{36}^{(k)}\gamma_{xy} \\
\sigma_{yz}^{(k)} &= \bar{Q}_{44}^{(k)}\gamma_{yz} + \bar{Q}_{45}^{(k)}\gamma_{xz} \\
\sigma_{xz}^{(k)} &= \bar{Q}_{54}^{(k)}\gamma_{yz} + \bar{Q}_{55}^{(k)}\gamma_{xz} \\
\sigma_{xy}^{(k)} &= \bar{Q}_{61}^{(k)}\epsilon_{xx} + \bar{Q}_{62}^{(k)}\epsilon_{yy} + \bar{Q}_{63}^{(k)}\epsilon_{zz} + \bar{Q}_{66}^{(k)}\gamma_{xy}
\end{aligned} \tag{2}$$

The $\bar{Q}_{ij}^{(k)}$ are the k^{th} layer stiffness transformed to $0xyz$ coordinates. The kinetic and potential energy can be expressed as

$$K = \frac{1}{2}\int_0^L \int_0^A \int_0^H \varrho^{(k)} \left[\left(\frac{\partial u_x}{\partial t}\right)^2 + \left(\frac{\partial u_y}{\partial t}\right)^2 + \left(\frac{\partial u_z}{\partial t}\right)^2\right] dxdydz \tag{3}$$

$$\begin{aligned} P = \frac{1}{2}\int_0^H \int_0^L \int_0^A & \overline{Q}_{11}^{(k)}\epsilon_{xx}^2 + 2\overline{Q}_{12}^{(k)}\epsilon_{xx}\epsilon_{yy} + 2\overline{Q}_{16}^{(k)}\epsilon_{xx}\gamma_{xy} + 2\overline{Q}_{31}^{(k)}\epsilon_{zz}\epsilon_{xx} \\ & + 2\overline{Q}_{32}^{(k)}\epsilon_{zz}\epsilon_{yy} + 2\overline{Q}_{36}^{(k)}\epsilon_{zz}\gamma_{yx} + \overline{Q}_{33}^{(k)}\epsilon_{zz}^2 + \overline{Q}_{22}^{(k)}\epsilon_{yy}^2 + 2\overline{Q}_{26}^{(k)}\gamma_{xy}\epsilon_{yy} \\ & + \overline{Q}_{66}^{(k)}\gamma_{xy}^2 + \overline{Q}_{44}^{(k)}\gamma_{zy}^2 + 2\overline{Q}_{45}^{(k)}\gamma_{xz}\gamma_{yz} + \overline{Q}_{55}^{(k)}\gamma_{xz}^2]dxdydz \end{aligned} \tag{4}$$

Assuming the following boundary conditions on the bottom and top surfaces

$$\sigma_{zx}(x,y,0,t) = \sigma_{zy}(x,y,0,t) = \sigma_{zz}(x,y,0,t) = 0$$

$$\sigma_{zx}(x,y,H,t) = \sigma_{zy}(x,y,H,t) = 0$$

$$\sigma_{zz}(x,y,H,t) = -q(x,y,t)$$

the external load work can be evaluated as

$$A = \int_0^L \int_0^A q(x,y,t)u_z(x,y,H,t)dxdy \tag{5}$$

To obtain the actual displacement field, the Lagrangian principle is applied and requires that

$$\delta\left\{\int_0^t [K - P + A]dt\right\} = 0 \tag{6}$$

METHOD OF SOLUTION

Considering the multilayered plates, we have to discuss the displacement approximation in the direction transversal to the interfaces of different layers. In general, it can be written as

$$\begin{aligned} u_x(x,y,z,t) &= \sum_i Z_i(z)u_i(x,y,t) \\ u_y(x,y,z,t) &= \sum_i Z_i(z)v_i(x,y,t) \\ u_z(x,y,z,t) &= \sum_i Z_i(z)w_i(x,y,t) \end{aligned} \tag{7}$$

where $Z_i(z)$ are the basic functions and $u_i(x,y,t)$, $v_i(x,y,t)$, $w_i(x,y,t)$ are the approximation coefficients. In the case of perfect contact between different layers all components of displacements are continuous through the thickness of the plate. Focusing the attention now on the different layer interfaces and keeping in mind that for actual stress-strain state, the transversal shear and normal stresses σ_{zz}, σ_{xz}, σ_{zy} are continuous on different layer interfaces. We have to admit discontinuity of ϵ_{zz}, ϵ_{zx}, ϵ_{yz} on the interfaces. Concluding we can formulate the following features of the functions $Z_i(z)$

1. $Z_i(z)i = 1,2,\ldots$ are continuous for $0 < z < H$.
2. $[dZ_i(z)/dz]$ may suffer the disruption of the first kind on the interfaces between layers.

The second aspect to be discussed is the displacement approximation in directions x and y. The three-dimensional displacement approximation can be rewritten as

$$\begin{aligned} u_x(x,y,z) &= \sum_i \sum_j \sum_k u_{ijk}(t) Z_i(z) X_j^u(x) Y_k^u(y) \\ u_y(x,y,z) &= \sum_i \sum_j \sum_k v_{ijk}(t) Z_i(z) X_j^v(x) Y_k^v(y) \\ u_z(x,y,z) &= \sum_i \sum_j \sum_k w_{ijk}(t) Z_i(z) X_j^w(x) Y_k^w(y) \end{aligned} \tag{8}$$

The superscripts are used to point out that in a general way different functions are used for different displacement components approximation. Indeed considering any problem, we have to satisfy a certain type of boundary condition on the lateral sides, and the mathematical formulation of the limitations for different components of displacements of cause can be different. So we have to use different basic functions for their approximation. Considering the smoothness of this function, they are supposed to have continuous derivatives in every point of the intervals $0 \le x \le L$ and $0 \le y \le A$, because layers are homogeneous in x- and y-directions.

SPLINE APPROXIMATION

The polynomial spline functions were applied [1–5] to displacements approximation both in transversal and inplane coordinates. Let us consider the approximation in transverse direction first. Every layer is divided into a certain number of sublayers l_k, $k = 1,\ldots,n$, by the planes $z = z_i$, $i = 1,\ldots,N-1$, $0 < z_1 < \ldots < z_N = H$. Here

$$N = \sum_{k=1}^{n} l_k$$

is the total number of sublayers. The coordinates of the interlaminar plains are z_{I_s}, $s = 1,\ldots,n - 1$

$$I_s = \sum_{k=1}^{s} l_k$$

To satisfy the above requirements on displacements and deformations, the recurrent procedure for constructing special linearly independent spline functions was elaborated. These spline functions, designated as $Z_{m,i}(z)$, are of mth degree and possess the defect $k_1 = 1$ in the nodes z_i, $i \neq I_s$, $s = 1,\ldots,n - 1$ and the defect $k_2{:}m \geq k_2 \geq k_1$ in the nodes z_i, $i = I_s$, $s = 1,\ldots,n - 1$. If $k_2 = m$, then according to Equation (11), displacements can be $m - 1$ times continuously differentiated with respect to z on the intervals $z_{I_{s-1}} < z < z_{I_s}$, $s = 1,\ldots,n$, but their first derivatives can be discontinuous at $z = z_{I_s}$, $s = 1,\ldots,n - 1$. For the case $m \geq 2$, the proposed approximation gives continuous displacements through the thickness of a package, as well as continuous strains and stresses through the thickness of each physical layer. On the interlaminar planes, there are disruptions in the magnitudes of transversal strains and stresses also, but use of more and more dense division into sublayers the disruptions of transversal stresses can be made less than every prescribed value when the disruptions of transversal strains remain. The details of the recurrent procedure will be considered for the particular cases $k_2 = m$ and $k_2 = k_1 = 1$ in Appendix 1.

The next step is to approximate $u_x(x,y,z)$, $u_y(x,y,z)$, $u_z(x,y,z)$—with respect to x and y coordinates by use of local polynomial splines. Let us introduce two sets of the nodes $0 = x_0 < x_1 < \ldots < x_M = L$ and $0 = y_0 < y_1 < \ldots < y_P = A$ on x- and y-axes. Due to presupposed homogeneity of all the mechanical characteristics of a layer along x and y coordinates, the $u_i(x,y,t)$, $v_i(x,y,t)$, $w_i(x,y,t)$ functions in Equation (7) have to be continuously differentiated with respect to x and y coordinates.

Finally, the displacements can be introduced in the following form:

$$u_x(x,y,z,t) = \sum_{i=0}^{N_m} \sum_{k=0}^{P+m_2-1} \sum_{j=0}^{M+m_1-1} u_{ijk}(t) Z_{m,i}(z) \chi_{m_1,j}(x) \chi_{m_2,k}(y)$$

$$u_y(x,y,z,t) = \sum_{i=0}^{N_m} \sum_{k=0}^{P+m_2-1} \sum_{j=0}^{M+m_1-1} v_{ijk}(t) Z_{m,i}(z) \chi_{m_1,j}(x) \chi_{m_2,k}(y) \tag{9}$$

$$u_y(x,y,z,t) = \sum_{i=0}^{N_m} \sum_{k=0}^{P+m_2-1} \sum_{j=0}^{M+m_1-1} w_{ijk}(t) Z_{m,i}(z) \chi_{m_1,j}(x) \chi_{m_2,k}(y)$$

where $\{\chi_{m_1,j}(x)\}$ and $\{\chi_{m_2,k}(y)\}$ are the sets of linearly-independent spline functions of m_1- and m_2-degrees, accordingly. They are to have the defect $k = 1$ in all nodes. The procedure for their calculation follows from the general recurrent procedure at $k_2 = k_1 = 1$.

By use of Equation (9), one can calculate a three-dimensional field of displacements in a laminated rectangular plate at homogeneous or inhomogeneous boundary conditions, imposed on the six boundary surfaces. Particularly for a laminate as a whole there can be formulated free support, clamping, free-edge conditions, or a combination thereof. It is possible also to impose an individual set of boundary conditions for each ply in a laminate, or for a certain group of plies.

The clamped edge boundary conditions will be considered as an example. Let us denote the edges of a plate in the following order

$$\Gamma_1{:}0 < x < L \qquad y = 0 \qquad \Gamma_3{:}0 < x < L \qquad y = A$$

$$\Gamma_2{:}0 < y < H \qquad x = \mathrm{L} \qquad \Gamma_4{:}0 < y < H \qquad x = 0$$

Then

$$u_x(x,y,z,t) = u_y(x,y,z,t) = u_z(x,y,z,t) = \frac{\partial u_z(x,y,z,t)}{\partial n} = 0$$
$$x,y \in \Gamma_i \qquad i = 1,\ldots,4 \qquad 0 \le z \le H \tag{10}$$

where $n = x$ for $i = 2,4$ and $n = y$ for $i = 1,3$. Accordingly, the values of spline functions at the ends of the interval, which are represented in Appendix 1, can be obtained from Equation (9)

$$u_x(x,0,z,t) = \sum_{i=0}^{N_m} \sum_{j=0}^{M+m_1-1} u_{ij0}(t) Z_{m,i}(z) \chi_{m_1,j}(x)$$

$$u_x(0,y,z,t) = \sum_{i=0}^{N_m} \sum_{k=0}^{P+m_2-1} u_{i0k}(t) Z_{m,i}(z) \chi_{m_2,k}(y)$$

$$u_x(x,A,z,t) = \sum_{i=0}^{N_m} \sum_{j=0}^{M+m_1-1} u_{ij,P+m_2-1}(t) Z_{m,i}(z) \chi_{m_1,j}(x)$$

$$u_x(L,y,z,t) = \sum_{i=0}^{N_m} \sum_{k=0}^{P+m_2-1} u_{i,M+m_1-1,k}(t) Z_{m,i}(z) \chi_{m_2,k}(y)$$

To provide Equation (10) we are to let in Equation (9)

$$u_{ij0}(t) = u_{ij,P+m_2-1}(t) = 0 \qquad i = 0,\ldots,N_m \qquad j = 0,\ldots,M + m_1 - 1$$

$$u_{i0k}(t) = u_{i,M+m_1-1,k}(t) = 0 \qquad i = 0,\ldots,N_m \qquad k = 0,\ldots,P + m_2 - 1 \tag{11}$$

To modify Equation (9) by eliminating the terms corresponding to Equation (11), we shall first introduce the vectors of basic spline functions and unknown coefficients. The components of the vector of basic spline functions $\vec{X}(x,y,z)$ which correspond to Equation (9) are definite as follows:

$$\{\vec{X}(x,y,z)\}_{iM_u+k(M+m_1)+j+1} = Z_{m,i}(z)\chi_{m_1,j}(x)\chi_{m_2,k}(y)$$

$$i = 0,\ldots,N_m \qquad j = 0,\ldots,M + m_1 - 1$$

$$k = 0,\ldots,P + m_2 - 1 \qquad M_u = (M + m_1)(P + m_2)$$

The vectors of unknown coefficients

$$\{\vec{U},\vec{V},\vec{W}\}_{iM_u+k(M+m_1)+j+1} = (u_{ijk},v_{ijk},w_{ijk})$$

$$i = 0,\ldots,N_m \qquad j = 0,\ldots,M + m_1 - 1$$

$$k = 0,\ldots,P + m_2 - 1 \qquad M_u = (M + m_1)(P + m_2)$$

Now we can write instead of Equation (9)

$$u_x(x,y,z) = \vec{X}(x,y,z)\vec{U}^*$$

$$u_y(x,y,z) = \vec{X}(x,y,z)\vec{V}^*$$

$$u_z(x,y,z) = \vec{X}(x,y,z)\vec{W}^*$$

It was shown that to modify this approximation in order to satisfy the boundary conditions, we are to eliminate the components of the $\vec{X}(x,y,z)$ which corresponds to Equation (11) decreasing the number of degrees of freedom. The relation between the modified vector of spline functions $\vec{X}^u(x,y,z)$ and $\vec{X}(x,y,z)$ can be written as

$$\vec{X}^u(x,y,z) = \hat{C}_u\vec{X}(x,y,z)$$

To obtain the components of the nonsquare matrix, $\hat{C}_u$, we are to assume it is the single matrix and then to delete the following rows

$$\text{row number} = \left\{\begin{array}{ll} iM_u + j + 1 & \left\{\begin{array}{l} i = 0,\ldots,N_m \\ j = 0,\ldots,M + m_1 - 1 \end{array}\right. \\ iM_u + (P + m - 1) \times (M + m_1 - 1) + j + 1 & \left\{\begin{array}{l} i = 0,\ldots,N_m \\ j = 0,\ldots,M + m_1 - 1 \end{array}\right. \\ iM_u + k(M + m_1 - 1) + 1 & \left\{\begin{array}{l} i = 0,\ldots,N_m \\ k = 0,\ldots,P + m_2 - 1 \end{array}\right. \\ iM_u + k(M + m_1 - 1) + M + m_1 & \left\{\begin{array}{l} i = 0,\ldots,N_m \\ k = 0,\ldots,P + m_2 - 1 \end{array}\right. \end{array}\right\}$$

Similar procedures are to be applied to other displacement components and the required approximation which satisfies the boundary conditions can be written

$$\begin{aligned} u_x(x,y,z,t) &= \hat{C}_u\vec{X}(x,y,z)\vec{U}^*(t) \\ u_y(x,y,z,t) &= \hat{C}_v\vec{X}(x,y,z)\vec{V}^*(t) \\ u_z(x,y,z,t) &= \hat{C}_w\vec{X}(x,y,z)\vec{W}^*(t) \end{aligned} \tag{12}$$

The set of equations to obtain the vectors of the coefficients of spline approximation can be obtained substituting Equation (12) in Equations (1), (2), and (3) and satisfying Equation (9). This set of equations is given in Appendix 2. To solve the set of ordinary differential equations, the implicit Wilson's method is used. After the calculation of the vectors of unknown coefficients $\vec{U}(t)$, $\vec{V}(t)$, $\vec{W}(t)$ the displacements can be obtained using Equation (12) and then the strains and stresses by use of Equations (1) and (2).

STRESS WAVE PROPAGATION IN A LAMINATED PLATE UNDER PRESCRIBED SURFACE LOAD PULSE

The method is capable of calculating the response characteristics of a multilayered plate to a very short time loading and investigating the stress wave propagation through the thickness of the plate. Let us consider a two-dimensional problem of the dynamic bending of a laminated plate, presupposing that the plate is infinitely long in y-direction (cylindrical bending). The load is prescribed by the formula

$$q(x,t) = q_0Q(t)\beta(x)$$

where

$Q(t) = t/t_0$ at $t \leq t_0$, $2 - t/t_0$ at $t_0 < t < 2t_0$, 0 at $t \geq 2t_0$

$\beta(x) = [(x - L/2)^2 - \epsilon^2]^2/\epsilon^4$ at $|x - L/2| \leq \epsilon$, and 0 at $|x - L/2| > \epsilon$

Two typical plates are considered. The first is manufactured of a cross-ply graphite/epoxy composite with unidirectional monolayers. The material of a monolayer has the following characteristics: $E_1 = 1.94 \cdot 10^{11}$ N/m², $E_3 = 7.72 \cdot 10^9$ N/m², $\nu_{13} = 0.3$, $G_{13} = 4.21 \cdot 10^9$ N/m², $\varrho = 1.63 \cdot 10^3$ kg/m³ (subscript 1 corresponds to the direction of reinforcement in a monolayer). The second plate is manufactured of isotropic organic glass layers with characteristics: $E = 6 \cdot 10^{10}$ N/m², $\nu = 0.3$, $\varrho = 1.5 \cdot 10^3$ kg/m³, and adhesive polymeric layers with $E = 2.8 \cdot 10^9$ N/m², $\nu = 0.33$, $\varrho = 10^3$ kg/m³. The values $L = 1$ m, $H = 0.01$ m, $\epsilon = 0.02L$ are used.

The magnitudes of σ_{zz}/q_0 for three-ply laminates under short-time impulse loads are shown in Figures 2 and 3 for several consecutive time instants. The direction of motion of the input impulse is indicated by arrows, as well as the direction of motion of the impulses passing through and reflected by the interfaces, upper and bottom free surfaces. It is seen from Figure 2, that in the case of orthotropic three-ply laminate having [0/90/0] layer layup, distortion of the input impulse is negligible. There are no visible impulses reflected from the interfaces. This effect can be explained by the identity of transverse elastic characteristics of a monolayer, presupposed in this calculation. From the results shown in Figure 3, it is obvious that in the case of a strong inhomogeneity of elastic characteristics through the thickness of a laminate, it is possible to govern stress wave propagation process and, therefore, to find the optimum structure of a laminate, which provides best resistance against the prescribed short-time pressure impulse.

NUMERICAL SIMULATION OF THE IMPACT INTERACTION

The variational approach by use of the Lagrange function for the system impactor-target is developed. The condition of nonpenetration is imposed at the contact zone, i.e., the normal displacement of the plate surface is mismatched with the impactor surface normal displacement. The friction in tangential direction is not accounted for. The method is capable of calculating the contact force, the velocity of the impactor and the size of the contact zone as well as the stress-strain field in the multilayered target versus time.

Let us consider the 2-D problem of the rigid body transverse impact at the multilayered target (Figure 4). The impactor shape is prescribed by a smooth function $z' = f(x') = f(-x')$ in the local coordinate system $0'x'z'$. The width of the contact zone at the time instant t is $2\epsilon(t)$. The normal displacement of the impactor is $Y(t)$. The initial conditions of this function are as follows:

$$Y(0) = 0 \qquad \frac{dY}{dt}(0) = V_0$$

where V_0 is the initial velocity of the impactor, the nonpenetration condition can be formulated as follows:

$$\begin{aligned} &Y(t) + f(x - L/2) - u_z(x,H,t) = 0 \qquad |L/2 - x| \leq \epsilon(t) \\ &Y(t) + f(x - L/2) - u_z(x,H,t) > 0 \qquad |L/2 - x| > \epsilon(t) \end{aligned} \tag{13}$$

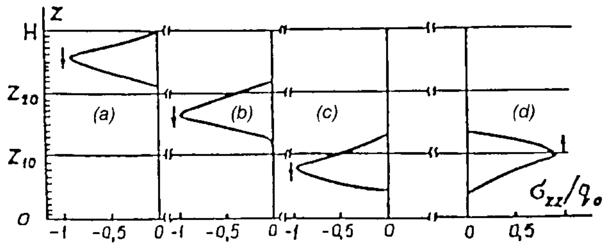

Figure 2. *Dependencies of transverse normal stress on Z-coordinate at the middle section of a [0°/90°/0°] graphite/epoxy plate at several time instants: $t = 2t_0$ (a), $4t_0$ (b), $6t_0$ (c), and $10t_0$ (d). t_0 = the loading time.*

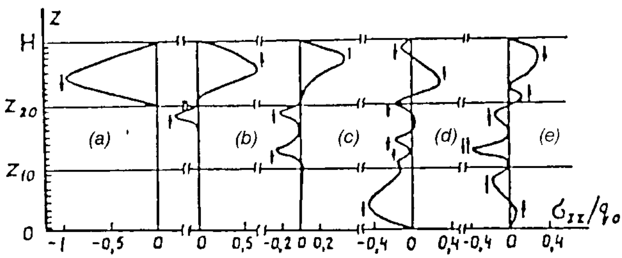

Figure 3. *Dependencies of transverse normal stress on Z-coordinate at the middle section of a three-ply organic glass/adhesive/organic glass plate at several time instants: $t = 2t_0$ (a), $4t_0$ (b), $8t_0$ (c), $11t_0$ (d), and $12t_0$ (e). t_0 = the loading time.*

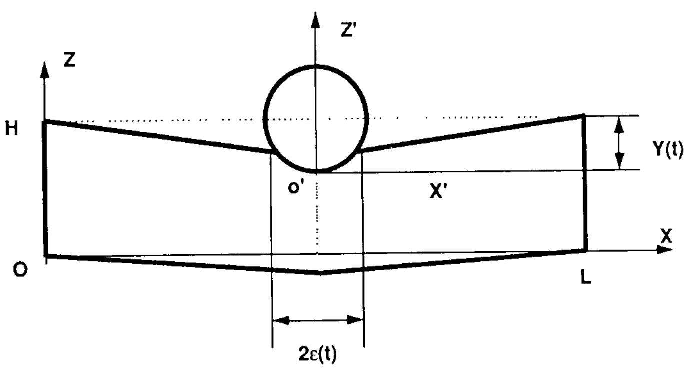

Figure 4. *Numerical simulation of impact interaction.*

The problem can now be formulated as a variational problem

$$\delta\left\{\int_0^t\left[K\left(\frac{d\vec{U}}{dt},\frac{d\vec{W}}{dt}\right) - P(\vec{U},\vec{W}) + \frac{1}{2}M\left(\frac{dY}{dt}\right)^2\right]dt\right\} = 0$$

under the conditions of Equation (13). Where the kinetic and potential energy are expressed through the coefficients of displacement approximation in directions x, z and M is the mass of impactor. To reduce the problem to the conditionless variational problem, we are to formulate Equation (13) in terms of spline functions. A possible formulation of the upper part of Equation (13) is

$$\int_{\frac{L}{2}-\epsilon}^{\frac{L}{2}+\epsilon}[Y(t) + f(x - L/2) - \hat{C}_w\vec{X}(x,H)\vec{W}^*]\vec{X}(x,H)dx = \vec{0} \qquad (14)$$

According to Equation (14) the discrepancy between normal displacement of the plate surface and the surface of impactor is orthogonal to all basic spline functions at the surface $z = H$. Using the Lagrange multiplier $\vec{\lambda}(t)$ we can formulate the following conditionless variational problem

$$\delta\int_0^t\left\{K\left(\frac{d\vec{U}}{dt},\frac{d\vec{W}}{dt}\right) - P(\vec{U},\vec{W}) + \frac{1}{2}M\left(\frac{dY}{dt}\right)^2\right.$$

$$\left. + \vec{\lambda}^*(t)\int_{\frac{L}{2}-\epsilon}^{\frac{L}{2}+\epsilon}[Y(t) + f(x - L/2) - \hat{C}_w\vec{X}(x,H)\vec{W}^*]\vec{X}(x,H)dx\right\}dt = 0$$

To derive the equations for obtaining the coefficients of spline approximation, the displacement of impactor and contact zone width, you must take the complete first variation of this functional and impose the independent terms to be zero. This set of equations is given in Appendix 3. It follows that the contact pressure at the contact zone can be evaluated as

$$q(x,t) = \vec{X}(x,H)\vec{\lambda}^*(t) \qquad |L/2 - x| < \epsilon(t) \qquad (15)$$

and the contact force

$$F(t) = \int_{\frac{L}{2}-\epsilon}^{\frac{L}{2}+\epsilon}\vec{X}(x,H)\vec{\lambda}^*(t)dx \qquad (16)$$

To obtain the contact zone width the following equation is to be applied

$$q[L/2 \pm \epsilon(t), t] = 0 \tag{17}$$

The solution procedure is based on the simultaneous step by step integration of equations for the plate under the load [Equation (15)] and the equation for impactor displacement under the force [Equation (17)] using implicit Wilson's method. To satisfy Equations (14) and (15) for obtaining the contact pressure and contact zone width, an iterational procedure was elaborated.

IMPACT CONTACT FORCE VERSUS TIME FOR DIFFERENT VELOCITIES AND MASS OF IMPACTOR

Let us consider low velocity rigid body impact on a rectangular plate assembled of graphite/epoxy unidirectional reinforced layers (fiber GY70) having the following elastic characteristics [6]:

$$E_1 = 102.1 \text{ GPa} \qquad E_3 = 6.96 \text{ GPa} \qquad G_{13} = 4.16 \text{ GPa}$$

$$\nu_{13} = 0.318 \qquad \varrho = 1630 \text{ kg/m}^3$$

Geometric parameters are $L = 0.2$ m, $A = 0.01$ m and $H = 0.01$ m. All the layers in a laminate are of equal thickness. The lay-up is [0/90/0] (fiber in the upper layer is oriented along the x-axis). All the numerical examples were calculated for impact energy in the range of 1.96–2.46 J. As it is seen from Figures 5–8, the dependency of contact force $F(t)$ is sharply different between a combination of small mass and high velocity and that of a large mass and very low velocity. According to Figure 5 in the case of heavy impactor the $F(t)$ function can be represented in a form of superposition of a sinusoidal function.

$$P(t) = P_0 \sin(\pi t/t_0)$$

where $t_0 = 0.0182$ sec, and short-period oscillations. The period of these oscillations is directly related to the time t_H of stress wave propagation through the thickness of a plate. The $P(t)$ function of both the parameters P_0 and t_0 can be evaluated exactly from a very simple energetic consideration [12]. By comparing $F(t)$, dependencies presented in Figure 6 for three pairs of M and V_0 one can conclude that repeated impacts are typical for contact interaction process at rather small mass and high velocity. It is interesting that the duration of the individual collisions and the time intervals between the subsequent collisions are practically independent of the mass and velocity values. Let us note also one general trend. If M value increases and, along with this, V_0 value decreases (impact energy preserves constant) than the absolute maximum of $F(t)$ corresponds to the second, third, and subsequent peaks on $F(t)$ curve. This tendency is valid up to certain M value at which separate collisions cannot be distinguished and they form "background" on which global plate deformation develops (see Figure 5).

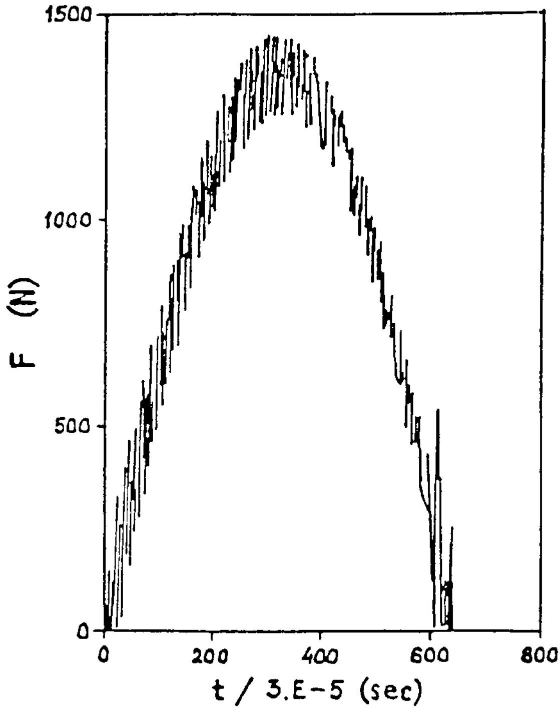

Figure 5. *Dependency of contact force on time for* $M = 17$ *kg,* $V_0 = 0.48$ *m/sec.*

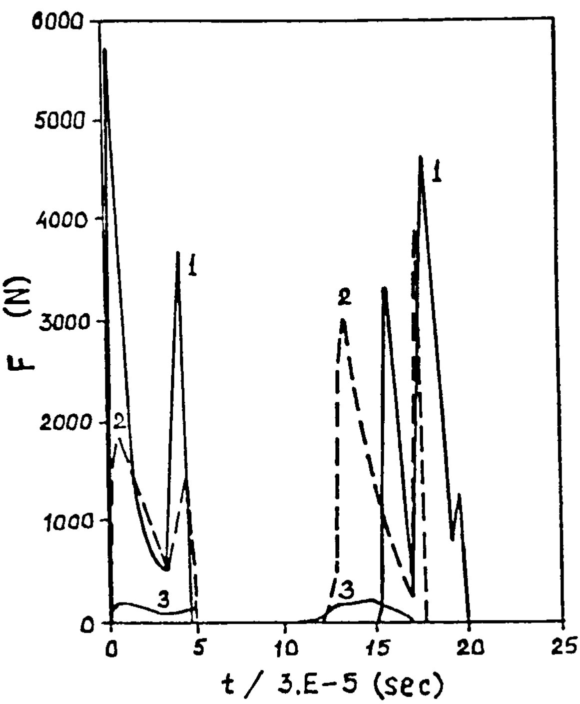

Figure 6. *Dependency of contact force on time for M = 25 g,* V_0 *= 13.5 m/sec (1); M = 0.2 g,* V_0 *= 4.5 m/sec (2); M = 17 kg,* V_0 *= 0.48 m/sec (3).*

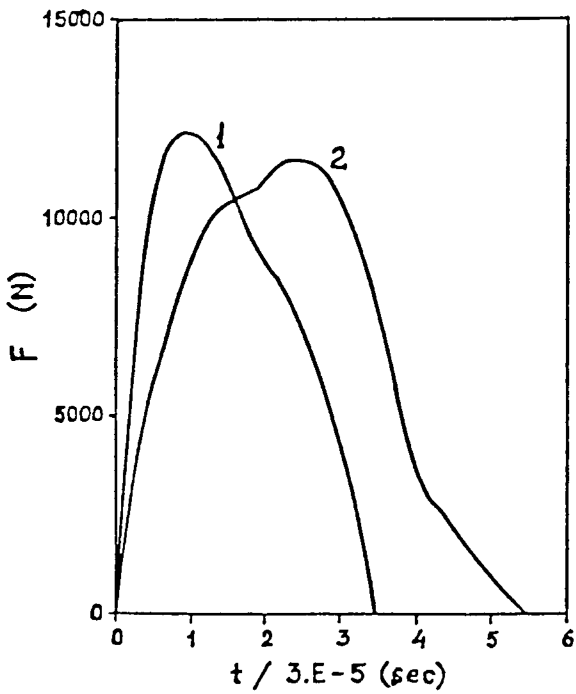

Figure 7. *Dependency of contact force on time for $M = 1$ g, $V_0 = 70$ m/sec (1); $M = 3$ g, $V_0 = 40.5$ m/sec (2).*

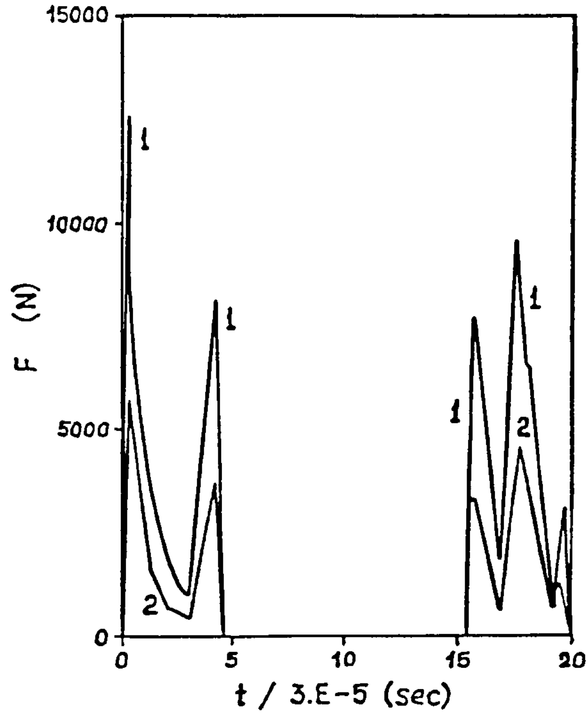

Figure 8. *Dependency of contact force on time for M = 25 g, V_0 = 27 m/sec (1); M = 25 g, V_0 = 13.5 m/sec (2).*

At very small M values according to Figure 7, the $F(t)$ peak corresponds to time values less than $2t_H$ and the peak value itself increases. The influence of V_0 value on $F(t)$ at constant M is illustrated in Figure 8. It can be seen that twice the enlargement in V_0 results in twice the enlargement in $F(t)$ peak values. However, the duration of the first and the second collisions and the time interval between these collisions do not change.

ANALYSIS OF IMPACT DAMAGE ZONES

The method can calculate all the components of displacement vector, strain and stress tensors in arbitrary point inside the volume of laminated plate during the whole impact event. The calculated values can be compared to their ultimate values at each step of numerical integration procedure. Let us designate $R_1^\pm$, $R_3^\pm$, and R_τ the ultimate strength values for unidirectional reinforced lamina in the direction of fibers, in the transverse direction, and in shear deformation, respectively (the sign "+" corresponds to tension, "−" to compression). If any stress component at some point inside a plate reaches its ultimate value, this point is marked on the two-dimensional map of impact damages. On the following figures (9 and 10) the damage zone corresponding to $\sigma_{11} \geq R_1^+$ condition is marked by dots, the zone corresponding to $\sigma_{33} \leq -R_3^-$ by the color black, corresponding to $\sigma_{33} \geq R_3^+$ by vertical shade and corresponding to $|\sigma_{13}| \geq R_\tau$ condition by oblique shade. By use of maximum stress criterion (as well as any other phenomenological strength criterion) we can correctly determine only one point on the map of damages. After each of the failure events, we first reduce certain stiffness characteristics of a lamina and, therefore of a package as a whole. Secondly, we are to take into account local overstress in the vicinity of each damage. Such a calculation needs a much more perfect procedure than we now have. But we can get certain useful information about damage zones (particularly, general trends of development, their final extent and moreover, intersections of zones corresponding to different failure modes). The "final" maps of damage zones are plotted in Figures 9 and 10 without taking into account any changes in stiffness characteristics and local overstresses. These "final" maps contain the largest damage zone for each failure mode calculated during the whole impact event. The calculations were performed for the laminate structure [0/90/0] at the following strength characteristics [12]: $R_1^+ = 230$ MPa, $R_3^+ = 20.7$ MPa, $R_3^- = 186$ MPa, $R_\tau = 59.3$ MPa. The time instants pointed out in Figures 5 and 6 correspond to the largest damage zones during the whole impact event. It can be noted that for heavy impactor the most dangerous mode of failure is fiber breakage on the back surface. At $M = 25$ g, there is a zone of internal transverse shear cracks (rather small at $V_0 = 13.5$ m/sec and much more extended, going through all the plies at $V_0 = 27$ m/sec). In the case of $M = 1$ g and $V_0 = 70$ m/sec there are two partly intersecting zones of transversal shear and normal tension cracks. In such a situation the spalling-type failure seems to be the most probable. Let us also note that at $V_0 = 27$ m/sec [Figure 9, (c)–(e)] there is a small zone in the vicinity of impactor where σ_{zz} magnitudes exceed the R_3^- ultimate value. Therefore, starting from this velocity value it is necessary to take into account the local plasticity of material in the region close to the place of impact.

In Reference [3] it was shown theoretically that the introduction of thin polyurethane interleaves between adjacent plies of graphite/epoxy composite can be a very effective method of stress state managing in a plate. Let us consider the results obtained for the same [0/90/0] laminate, but having two different isotropic material interleaves between 0 and 90 layers. The first material (designated further as R1) has the following characteristics: $E = 1.6$ GPa, $\nu = 0.4$, $\varrho = 1400$ kg/m^3, $R^+ = 39.9$ MPa, $R^- = 62.5$ MPa. The second material (accordingly, R2) has the following characteristics: $E = 0.7$ GPa, $\nu = 0.43$, $\varrho = 1238$ kg/m^3, $R^+ = 93.1$ MPa, $R^- = 144.8$ MPa. Both the types of interleaves have 1 mm thickness. The structures of five-ply laminates can be designated as [0/R1/90/R1/0] and [0/R2/90/R2/0] accordingly. The results of the same loading conditions as for Figure 9 are presented in Figure 10. The comparison of Figures 9 and 10 leads to the conclusion that not only the presence of interleaves is important, but also the ratio between E and R^+ values. The effect of interleaves is rather different for the materials R1 and R2. In the case of spalling-type failure mode, the introduction of the interleaves of material R2 leads to separation of the failure zones in different layers [compare Figures 9(d) and 10(d)] and makes more likely

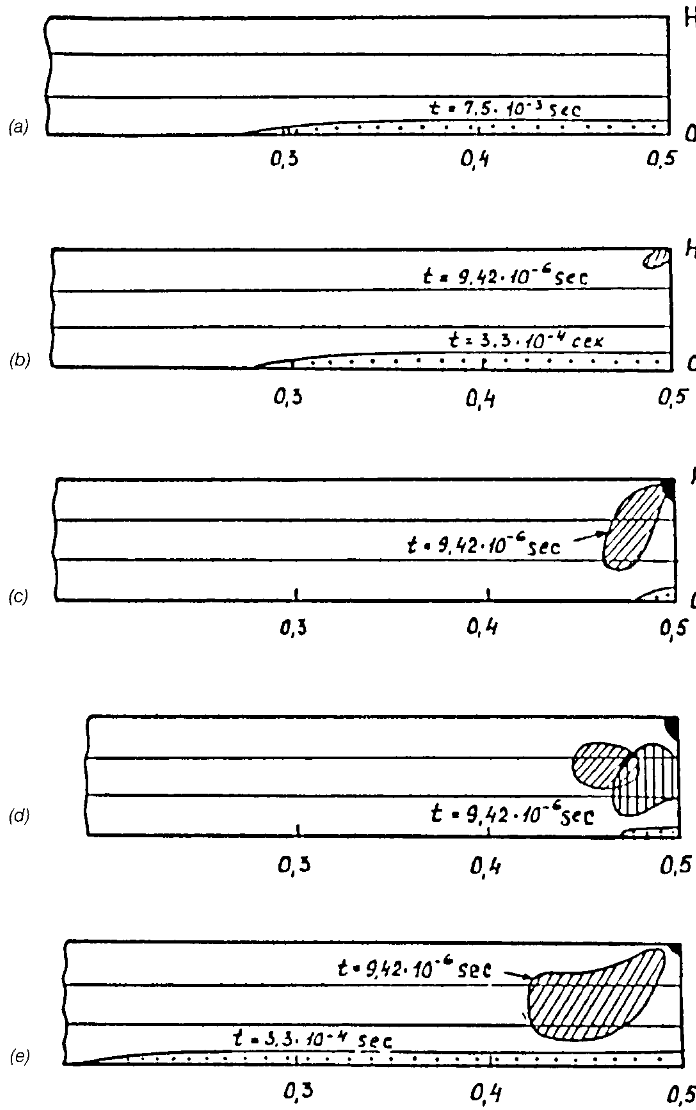

Figure 9. *Impact damage zones for three-ply laminates at $M = 17$ kg, $V_0 = 0.48$ m/sec (a); $M = 25$ g, $V_0 = 13$ m/sec (b); $M = 3$ g, $V_0 = 40.5$ m/sec (c); $M = 1$ g, $V_0 = 70$ m/sec (d); $M = 25$ g, $V_0 = 25$ m/sec (e).*

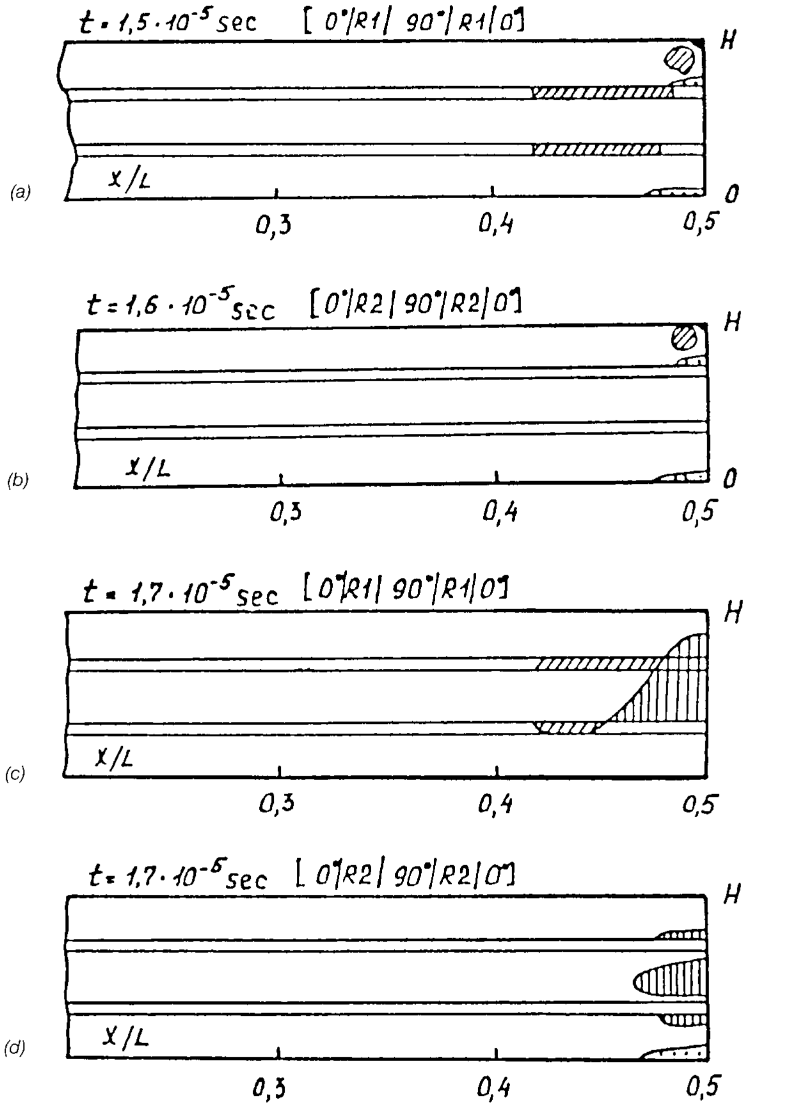

Figure 10. *The same for five-ply laminates at $M = 3$ g, $V_0 = 40.5$ m/sec [(a) and (b)]; $M = 1$ g, $V_0 = 70$ m/sec [(c) and (d)].*

the internal spalling damage of either of the material pull-outs from the bottom surface.

CONCLUSIONS

A numerical method for the calculation of the dynamic response characteristics in a multilayered plate is proposed. The method is based on displacement spline approximation and is capable of calculating stress-strain fields in composites subjected to a very short time loading. The stress wave propagation through the thickness of three-layered isotropic and cross-ply graphite/epoxy plates was investigated. To provide the redistribution of the amplitude of the stress impulse passing through the thickness of a composite, a soft interleave between layers was examined.

A low-velocity impact by a rigid body on a multilayered plate was considered. To describe the impact interaction, a variational formulation of dynamic contact problem was developed. The general conclusion from the analysis performed in this paper is that the parameters of impact contact interaction and the characteristics of stress state in a plate are very sensitive to both the velocity and the mass of impactor at the given impact energy value. Different modes of failure in composites can be realized, depending on the mass and velocity of impactor. At the level of rather high velocities and small mass, the spalling-type failure is revealed. To prevent the material pull-out of redistributing the normal tensile stresses, different types of soft interleaves between layers are examined. Maximum efficiency performs thus with maximum strength-stiffness ratio.

APPENDIX 1

The recurrent procedure will be considered for the particular cases $k_2 = m$ and $k_2 = k_1 = 1$, the case when $k_2 = k_1 = 1$ corresponds to a single-ply plate. At $m = 1$, the approximation of displacements is carried out by means of piecewise-linear standard "cap" splines (Figure A1.1). The higher order basic functions can be calculated by use of successive integration of $Z_{1,i}(z)$-functions in accordance with the formulas

$$F_{m,i}(z) = \int_0^z Z_{m-1,i}(z)dz \qquad F_{m,-1}(z) \equiv 1$$
$$i = 0,1,\ldots,N + m - 2 \qquad m = 2,3,\ldots \tag{A1.1}$$

These functions do not possess a local supporter, therefore it is purposeful to introduce into consideration their linear combinations:

$$Z_{m,i}(z) = \frac{F_{m,i-1}(z)}{F_{m,i-1}(z_N)} - \frac{F_{m,i}(z)}{F_{m,i}(z_N)} \qquad i = 0,1,\ldots,N + m - 1 \tag{A1.2}$$

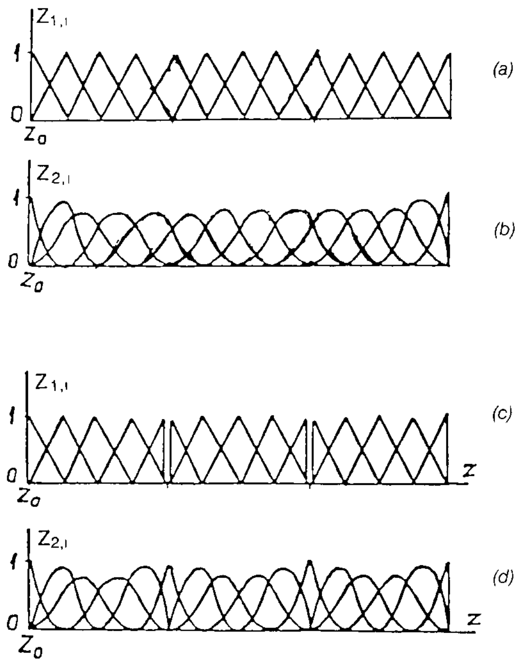

Figure A1.1. *The $Z_{m,i}$ splines at $N = 12$ for $k_1 = k_2 = 1$ [(a) and (b)] and for $k_1 = 1$, $k_2 = 1$ [(c) and (d)].*

The functions $Z_{2,i}(z)$, obtained by application of the Formulas (A1.1) and (A1.2) to $Z_{1,i}(z)$, are presented in Figure A1.1(b).

For the splines with $k_2 = m$ which we need to approximate displacements in a laminate, the same idea about subsequent integration of the first-degree basic functions is used. Let us consider displacement, u_x, omitting further, all the arguments, except z. The desired mth degree spline approximation can be written as

$$u_x(z) = \sum_i u_i Z_{m,i}(z) \tag{A1.3}$$

From the condition $k_2 = m$, it follows that the function $\partial u_x / \partial z$ is discontinuous at $z = z_{l_s}$, $s = 1, \ldots, n - 1$. We can approximate this function in the following way

$$\frac{\partial u_x}{\partial z} = \sum_{i=0}^{l_s+m-1} u_i^{(s)} Z_{m-1,i}^{(s)}(z) \qquad s = 1, \ldots, n \tag{A1.4}$$

The sets of spline functions $\{Z^{(s)}_{m-1,i}\}_{i=0}^{l_s+m-1}$ are defined on intervals $z_{I_{s-1}} < z < z_{I_s}$, $s = 1,\ldots,n$ and possessing the defect $k_1 = 1$ in the nodal points inside the intervals. On each interval they can be obtained applying $m - 2$ times [Equations (A1.1) and (A1.2)] to the first degree "cap" functions replacing z_0, z_N, N for $z_{I_{s-1}}$, z_{I_s}, l_S accordingly. To get the desired approximation [Equation (A1.3)], we are to apply one more time Equations (A1.1) and (A1.2) to Equation (A1.4) but on the whole interval. The first degree splines to get the second degree spline approximation when $k = 2$ for $z = z_{I_1}$, z_{I_2}, z_{I_3} and $k = 1$ in other nodal points are shown in Figure A1.1(c). The resulting second degree splines are represented in Figure A1.1(d).

The following features of the spline functions at the ends of the intervals can be established

$$Z_{m,0}(0) = Z_{m,N_m}(H) = 1 \qquad Z_{m,i}(0) = Z_{m,i}(H) = 0 \qquad i = 1,N_m$$

where $N_m = N + m - 1$.

APPENDIX 2

$$\hat{C}_u[\hat{D}^{11}_{xx} + \hat{D}^{16}_{xy} + \hat{D}^{16}_{yx} + \hat{D}^{66}_{yy} + \hat{D}^{55}_{zz}]\hat{C}_u^{*}\vec{U} + \hat{C}_u[\hat{D}^{16}_{xx} + \hat{D}^{12}_{xy} + \hat{D}^{66}_{yx} + \hat{D}^{26}_{yy} + \hat{D}^{45}_{zz}]\hat{C}_v^{*}\vec{V} + \hat{C}_u[\hat{D}^{31}_{xz} + \hat{D}^{45}_{zy} + \hat{D}^{36}_{yz} + \hat{D}^{55}_{zx}]\hat{C}_w^{*}\vec{W} = \hat{C}_u\hat{D}_\rho\hat{C}_u\frac{d^2\vec{U}}{dt^2}$$

$$\hat{C}_v[\hat{D}^{16}_{xx} + \hat{D}^{66}_{xy} + \hat{D}^{12}_{yx} + \hat{D}^{26}_{yy} + \hat{D}^{45}_{zz}]\hat{C}_u^{*}\vec{U} + \hat{C}_v[\hat{D}^{66}_{xx} + \hat{D}^{26}_{xy} + \hat{D}^{26}_{yx} + \hat{D}^{22}_{yy} + \hat{D}^{44}_{zz}]\hat{C}_v^{*}\vec{V} + \hat{C}_v[\hat{D}^{36}_{xz} + \hat{D}^{44}_{zy} + \hat{D}^{32}_{yz} + \hat{D}^{45}_{zx}]\hat{C}_w^{*}\vec{W} = \hat{C}_v\hat{D}_\rho\hat{C}_v\frac{d^2\vec{V}}{dt^2}$$

$$\hat{C}_w[\hat{D}^{55}_{xz} + \hat{D}^{36}_{zy} + \hat{D}^{45}_{yz} + \hat{D}^{31}_{zx}]\hat{C}_u^{*}\vec{U} + \hat{C}_w[\hat{D}^{45}_{xz} + \hat{D}^{32}_{zy} + \hat{D}^{44}_{yz} + \hat{D}^{36}_{zx}]\hat{C}_v^{*}\vec{V} + \hat{C}_w[\hat{D}^{11}_{xx} + \hat{D}^{16}_{xy} + D^{16}_{yx} + \hat{D}^{66}_{yy} + \hat{D}^{33}_{zz}]\hat{C}_w^{*}\vec{W} = \hat{C}_w\int_0^A dy\int_0^L q(x,y)\vec{X}(x,y,H,t)\,dx + \hat{C}_w\hat{D}_\rho\hat{C}_w\frac{d^2\vec{W}}{dt^2}$$

The following matrices are used in these equations:

$$\{\hat{D}^{kl}_{\alpha\beta}\}_{ij} = \int_0^H \bar{Q}_{kl}(z)\int_0^A\int_0^L \frac{\partial\{\vec{X}(x,y,z)\}_i}{\partial\alpha}\,\frac{\partial\{\vec{X}(x,y,z)\}_j}{\partial\beta}\,dxdydz$$

$$\alpha,\beta = x,y,z \qquad k,l = 1,\ldots,6$$

$$\{\hat{D}_\rho\}_{ij} = \int_0^H \varrho(z) \int_0^A \int_0^L \{\vec{X}(x,y,z)\}_i \{\vec{X},x,y,z)\}_j dxdydz$$

$$i,j = (M + m_1)(P + m_2)(N_m + 1)$$

The $\overline{Q}_{ij}(z)$ and $\varrho(z)$ are the pice-vice constant functions defined as follows:

$$\overline{Q}_{ij}(z) = \overline{Q}_{ij}^{(k)} \qquad \varrho(z) = \varrho^{(k)}$$

$$i,j = 1,\ldots,6 \quad \text{for} \quad z_{I_{k-1}} < z < z_{I_k} \qquad k = 1,\ldots,n$$

APPENDIX 3

$$\hat{C}_u[\hat{D}_{xx}^{11} + \hat{D}_{zz}^{55}]\hat{C}_u^*\vec{U} + \hat{C}_u[\hat{D}_{xz}^{31} + \hat{D}_{zx}^{55}]\hat{C}_w^*\vec{W} = \hat{C}_u\hat{D}_\rho\hat{C}_u^*\frac{d^2\vec{U}}{dt^2} \tag{A3.1}$$

$$\hat{C}_w[\hat{D}_{xz}^{55} + \hat{D}_{zx}^{31}]\hat{C}_u^*\vec{U} + \hat{C}_w[\hat{D}_{xx}^{11} + \hat{D}_{zz}^{33}]\hat{C}_w^*\vec{W}$$

$$= \hat{C}_w \int_{\frac{L}{2}-\epsilon}^{\frac{L}{2}-\epsilon} [\vec{\lambda}^*(t)\vec{X}(x,H)]\vec{X}(x,H)dx + \hat{C}_w\hat{D}_\rho\hat{C}_w^*\frac{d^2\vec{W}}{dt^2} \tag{A3.2}$$

$$M\frac{d^2Y}{dt^2} = \int_{\frac{L}{2}-\epsilon}^{\frac{L}{2}+\epsilon} [\vec{\lambda}^*(t)\vec{X}(x,H)]dx \tag{A3.3}$$

$$\vec{\lambda}^*(t)\vec{X}\left(\frac{L}{2} \pm \epsilon, H\right) = 0 \tag{A3.4}$$

The equations were derived imposing the partial variations on $\vec{U}(t)$, $\vec{W}(t)$, $Y(t)$, $\epsilon(t)$ to be zero. To complete this set, the conditions of nonpenetrating [Equation (14)] are required. The matrices in Equations (A3.1) and (A3.2) are similar to that defined in Appendix 2.

REFERENCES

1. Bogdanovich, A. E. and E. V. Yarve. 1983. "Stress Analysis in Multilayered Beams under Transverse Dynamic Bending," *Mechanics of Composite Materials* (in Russian), translated by Consultant Bureau. New York: Plenum Publishing Corporation, (5):824–837.
2. Bogdanovich, A. E. and E. V. Yarve. 1988. "Numerical Solution of the Two-Dimensional Tran-

sient Deformation Problem for a Laminated Media," *Mechanics of Composite Materials* (in Russian), translated by Consultant Bureau. New York: Plenum Publishing Corporation, (1):36–44.

3. Bogdanovich, A. E. and E. V. Yarve. 1989. "Numerical Analysis of Impact Deformation of Composite Plates," *Mechanics of Composite Materials* (in Russian), translated by Consultant Bureau. New York: Plenum Publishing Corporation, (5):804–820.
4. Bogdanovich, A. E. and E. V. Yarve. 1989. "Calculation of Stresses in Laminated Materials under Transverse Bending," *Proceedings of the Second International Symposium on Brittle Matrix Composites, Cedzyna, Poland, Sept. 20–22, 1988*, Elsevier Applied Science, pp. 658–672.
5. Bogdanovich, A. E. and E. V. Yarve. 1989. "Numerical Analysis of Laminated Composite Plates Subjected to Impact Loading," *Proceedings of the American Society for Composites, Fourth Technical Conference*, pp. 399–409.
6. Greszszuk, L. B. 1982. "Damage in Composite Materials Due to Low Velocity Impact," *Impact Dynamics*. John Wiley and Sons, Inc., pp. 55–94.
7. Yang, S. H. and C. T. Sun. 1982. "Indentation Law for Composite Laminates," *Composite Materials: Testing and Design, Sixth Conference, ASTM STP 787*, pp. 425–449.
8. Tan, T. M. and C. T. Sun. 1985. "Wave Propagation in Graphite/Epoxy Laminates Due to Impact," *Journal of Applied Mechanics*, 52:6–12.
9. Sun, C. T. and J. K. Chen. 1985. "On the Impact of Initially Stressed Composite Laminates," *Journal of Composite Materials*, 19:490–504.
10. Leicy, D. and P. J. Hogg. 1989. "The Effect of Crystallinity on the Impact Properties of Advanced Thermoplastic Composites," *Developments in the Science and Technology of Composite Materials, Third European Conference*, pp. 809–815.
11. Gulidov, A. I. and I. I. Shabalin. 1987. "Numerical Realization of Boundary Conditions in Dynamic Contact Problems," *Institute of Theoretical and Applied Mechanics, Preprint* (in Russian), Novosibirsk, p. 37.
12. Kravchuk, A. S. 1985. "Variational Method in Dynamic Contact Problems," *Mechanics of Deformable Bodies and Structures, School Seminar on the Theory of Elasticity and Visco-Elasticity* (in Russian), Erevan, pp. 235–241.
13. Lee, J. D., S. Du and H. Liebovitz. 1984. "Three-Dimensional Finite Element and Dynamic Analysis of Composite Laminate Subjected to Impact," *Computers and Structures*, N5/6: 807–813.
14. Wu, H. T. and G. S. Springer. 1988. "Impact Induced Stresses, Strains and Delaminations in Composite Plates," *Journal of Composite Materials*, 22:533–560.
15. Bachrach, W. E. 1988. "Impact Damage in Composite Laminates," *Proceedings of the 4th Japan-U.S. Conference on Composite Materials*, pp. 53–62.
16. Hsi-Yung, T. Wu and F.-K. Chang. 1989. "Transient Dynamic Analysis of Laminated Composite Plates Subjected to Transverse Impact," *Computers and Structures*, N3:453–466.
17. Wu, H. T. and G. S. Springer. 1988. "Measurements of Matrix Cracking and Delamination Caused by Impact on Composite Plates," *Journal of Composite Materials*, 22:518–532.